

The role of nonthermal electrons in the optical continuum of stellar flares

M. D. Ding and C. Fang

Department of Astronomy, Nanjing University, Nanjing 210093, China

Accepted 2000 . Received 2000 ; in original form 2000

ABSTRACT

The continuum emission of stellar flares in UV and visible bands can be enhanced by two or even three orders of magnitude relative to the quiescent level and is usually characterised by a blue colour. Thermal atmospheric models are difficult to reproduce all these spectral features. If the flaring process involves the acceleration of energetic electrons which then precipitate downwards to heat the lower atmosphere, collisional excitation and ionisation of ambient hydrogen atoms by these nonthermal electrons could be important in powering the continuum emission. To explore such a possibility, we compute the continuum spectra from an atmospheric model for a dMe star, AD Leo, at its quiescent state, when considering the nonthermal effects by precipitating electron beams. The results show that if the electron beam has an energy flux large enough (for example, $\mathcal{F}_1 \sim 10^{12} \text{ erg cm}^{-2} \text{ s}^{-1}$), the U band brightening and, in particular, the $U-B$ colour are roughly comparable with observed values for a typical large flare. Moreover, for electron beams with a moderate energy flux $\mathcal{F}_1 \lesssim 10^{11} \text{ erg cm}^{-2} \text{ s}^{-1}$, a decrease of the emission at the Paschen continuum appears. This can explain at least partly the continuum dimming observed in some stellar flares. Adopting an atmospheric model for the flaring state can further raise the continuum flux but it yields a spectral colour incomparable with observations. This implies that the nonthermal effects may play the chief role in powering the continuum emission in some stellar flares.

Key words: stars: activity – stars: atmospheres – stars: flare – stars: late-type.

1 INTRODUCTION

Flares have been detected in stars of various types. In particular, very energetic flares are likely to occur in dKe/dMe stars. The most energetic stellar flare can release an energy as large as $\sim 10^{35}$ erg in total, three orders of magnitude greater than that in the biggest flare on the Sun (see e.g. Pagano et al. 1997). Multiwavelength observing campaigns have been made to detect flare emissions in different wavelength regions like the soft X-ray, EUV, optical, and radio and then to quantify their relationships (e.g. Hawley & Pettersen 1991; Hawley et al. 1995; van den Oord et al. 1996). Though, there are still few hard X-ray observations of stellar flares.

In spite of many different aspects between stellar and solar flares (Haisch, Strong & Rodonò 1991), they may share similarities in some basic physical processes, such as the energy release process, heating of the atmosphere, and origin of the continuum and line emissions. The well-known solar flare model assumes that a flare is produced through the reconnection of magnetic field lines, leading to the formation of a current sheet where tearing mode instability occurs.

This process releases a large amount of thermal energy and results in an acceleration of electrons and/or protons. Accelerated electrons then impact the lower atmosphere, producing hard X-ray emission through bremsstrahlung, and causing an enhancement of optical continuum and line emissions (e.g. Neidig et al. 1993). Meanwhile, the corona accumulates material evaporated from the chromosphere when heated by nonthermal electrons and the soft X-ray flux gradually increases. The ‘Neupert effect’, assuming that the soft X-ray flux is proportional to the time integral of hard X-ray flux, is found valid not only for solar flares (Dennis & Zarro 1993), but also for stellar flares if using optical data as a proxy for hard X-ray emission (Hawley et al. 1995).

The UV and optical continuum in stellar flares is found to exhibit several emission features. First, the continuum is usually characterised by a blue colour. Pagano et al. (1997) found in an intense flare a very blue emission ($U - B \approx -2.5$), implying a significant enhancement of the Balmer continuum and a flare site close to the stellar limb. A blue continuum was also observed by Hawley & Fisher (1992), which was reproduced from atmospheric models proposed by Mauas & Falchi (1996), taking into account the merging

arXiv:astro-ph/0005388v1 19 May 2000

of higher Balmer lines. Second, some flares are preceded by a dimming in their continuum emission (e.g. Hawley et al. 1995). Several models have been proposed to explain such negative flares. Gurzadyan (1980) proposed inverse Compton up-conversion of ‘red’ photons to the U band by extremely energetic electrons. However, this model demands a total energy ($\sim 10^{40}$ erg) of energetic electrons which is unrealistically large (Hénoux et al. 1990). Mullan (1975) suggested that the dips in the red light curve can be produced by $H\alpha$ absorption. At present, the most favourable model is the H^- absorption model of Grinin (1983), which suggests that an energy input to the lower atmosphere leads to an enhanced H^- opacity and then reduces the photospheric continuum radiation.

The situation is more or less similar in solar white-light flares (WLFs), those flares emitting an enhanced optical continuum. The majority of solar WLFs exhibit a pronounced Balmer jump while a small fraction shows no jump, which are classified as type I and type II WLFs, respectively (Machado et al. 1986; Fang & Ding 1995). Recombination of hydrogen atoms in the chromosphere is responsible for the continuum emission in the first case while the H^- emission plays the main role in the second case. Besides, a negative continuum contrast is also theoretically predicted at the very beginning of flare occurrence (Hénoux et al. 1990; Ding & Fang 1996). Contrary to the stellar case, a negative solar WLF, the so-called black-light flare (BLF), is hard to observe due to its small amplitude of dimming and its short duration. In fact, no direct observational evidence has proved its existence (van Driel-Gesztelyi et al. 1994).

Since the lower atmosphere of flares is very likely to be heated through bombardment of energetic electrons, the nonthermal collisional excitation and ionisation of hydrogen atoms can be important in increasing the continuum opacity and source function (Hénoux, Fang & Gan 1993). The emergent continuum emission is then greatly enhanced and characterised by a Balmer jump. The continuum contrast depends on the flux and spectrum of the electron beam and also on the flare site (Ding & Fang 1996).

The atmospheric structure and, in particular, the parameters of the electron beam in stellar flares can be quite different from that in a solar flare. Thus, it is still unclear and needs to be quantified to what extent the nonthermal effects can alter the continuum emission in stellar flares. The purpose of this paper is to explore this question. To do so, we employ atmospheric models typical for dMe stars and do non-LTE calculations in the presence of an electron beam. The results show the role of nonthermal effects on the optical continuum and are useful in the spectroscopy of stellar flares.

2 COMPUTATIONAL METHOD

2.1 Atmospheric models

In last decades, attempts have been made to model the atmosphere of stars of different spectral types. Here, we restrict our attention to the work on late-type stars, in particular, M dwarfs, which have a lower effective temperature. The reason is that in such stars, the afore-mentioned nonthermal effects during flares may be relatively more significant.

Some early atmospheric models of dM or dMe stars were built on limited spectral data. Thus, their chromospheric structures are usually very schematic (e.g. Cram & Mullan 1979). Multi-line spectral data are needed for a better modelling of the stellar atmosphere. Recently, after constructing grids of atmospheric models and examining their different spectral features, methods for probing the atmosphere are being developed which use spectral lines including $H\text{I Ly}\alpha$, $H\alpha$ ($H\beta$), Ca II H (K) , Mg II h (k) , and Na I D lines etc. as well as continua (e.g. Doyle et al. 1994; Houdebine & Doyle 1994; Houdebine, Doyle & Kościelicki 1995; Houdebine et al. 1996; Houdebine & Stempels 1997; Short & Doyle 1998).

Mauas & Falchi (1994) presented a semi-empirical model for the dMe star AD Leo, which can reproduce both the continuum and most spectral lines from observations. Their model is elaborate especially in the chromospheric structure, though, there may be some uncertainties in the temperature minimum region, as they stated. Mauas & Falchi (1996) further constructed semi-empirical models for a large flare on AD Leo observed by Hawley & Pettersen (1991). They computed three models corresponding to different filling factors. Compared to the quiescent atmosphere, these models indicate a strong heating in both the chromosphere and the photosphere, which is quite different from the case of a solar flare. In particular, Mauas & Falchi (1996) discussed the possible role of high energy electrons on heating the deeper atmosphere.

2.2 Nonthermal excitation and ionisation rates of hydrogen by electron beams

Here we assume that the basic scenario for solar flares is still true for stellar flares, that is, flares originate in stellar coronae and involve the production of a beam of high energy electrons, streaming downward to heat the lower atmosphere. In the cold target approximation, the rate of energy loss for beam electrons with column density N has the form (Emslie 1978; Hénoux et al. 1993):

$$\frac{dE}{dN} = -\frac{K}{\mu E} \gamma = -\frac{K}{\mu E} [\xi \Lambda + (1 - \xi) \Lambda'], \quad (1)$$

where $K = 2\pi e^4$. In equation (1), μ is the cosine of the pitch angle, ξ is the ionisation degree of the target, Λ is the Coulomb logarithm due to collisions with target electrons and protons, while Λ' the one for inelastic collisions with target atoms. The latter corresponds to the energy deposit contributed to the nonthermal excitation and ionisation of target atoms. The rate of energy deposit at column density N through inelastic collisions is written as (Emslie 1978; Chambe & Hénoux 1979):

$$\Phi = \frac{dE}{dt} = (1 - \xi) n_H \Lambda' K \int_{E_N}^{\infty} \frac{F_0(E) dE}{E(1 - E_N^2/E^2)^{\frac{2+\beta}{4+\beta}}}, \quad (2)$$

where

$$E_N = \left[\left(2 + \frac{\beta}{2} \right) \frac{\gamma K N}{\mu_0} \right]^{\frac{1}{2}} \quad (3)$$

is the minimum energy of electrons that can penetrate to N . The cosine of the initial pitch angle, μ_0 , is taken to be unity throughout the paper. The expression for β can be found in Emslie (1978). Knowing little about the energy distribution

of the beam electrons, we assume a power law for the initial flux spectrum with a low-energy cut-off:

$$F_0(E) = \begin{cases} AE^{-\delta}, & E > E_1, \\ 0, & E < E_1, \end{cases} \quad (4)$$

where $A = (\delta - 2)\mathcal{F}_1 E_1^{\delta-2}$. \mathcal{F}_1 is the energy flux of electrons. Equation (2) then reduces to

$$\Phi = \frac{1}{2}(1-\xi)n_H\Lambda'K(\delta-2)\frac{\mathcal{F}_1}{E_1^2}\left(\frac{N}{N_1}\right)^{-\frac{\delta}{2}}\int_0^{u_1}\frac{u^{\frac{\delta}{2}-1}du}{(1-u)^{\frac{2+\beta}{4+\beta}}}, \quad (5)$$

where

$$N_1 = \frac{\mu_0 E_1^2}{(2 + \beta/2)\gamma K} \quad (6)$$

is the column density penetrated by particles with an initial energy E_1 , and

$$u_1 = \begin{cases} 1, & N > N_1, \\ N/N_1, & N < N_1. \end{cases} \quad (7)$$

In the present calculations, we adopt an atomic model for hydrogen with four bound levels plus continuum. According to Fang, Hénoux & Gan (1993), the nonthermal collisional excitation rates due to bombarding electrons from the ground state are derived as

$$C_{12}^B \simeq 2.94 \times 10^{10} \Phi / n_1, \quad (8)$$

$$C_{13}^B \simeq 5.35 \times 10^9 \Phi / n_1, \quad (9)$$

and

$$C_{14}^B \simeq 1.91 \times 10^9 \Phi / n_1, \quad (10)$$

and the nonthermal ionisation rate is

$$C_{1c}^B \simeq 1.73 \times 10^{10} \Phi / n_1. \quad (11)$$

These rates are then incorporated into the statistical equilibrium equations, which are solved iteratively together with the radiative transfer equation for a specific atmospheric model. Finally the continuum flux at the stellar surface is computed as

$$F_\lambda = 2\pi \int_0^1 I_\lambda(\mu)\mu d\mu = 2\pi \int_0^1 d\mu \int_0^\infty S_\lambda e^{-\tau_\lambda/\mu} d\tau_\lambda. \quad (12)$$

3 RESULTS AND DISCUSSIONS

Using the above method, we have studied the role of non-thermal electrons on the continuum emission in stellar flares. Since the flaring atmosphere undergoes a rapid evolution during the heating process, we consider two quasi-static cases (marked as A and B), an initial cool atmosphere and a heated atmosphere, which are assumed to be represented respectively by the atmospheric model for the quiescent state (Mauas & Falchi 1994) and that for a flaring state (Mauas & Falchi 1996, their model B) of the M dwarf AD Leo. This is reasonable as the radiative time scale is much shorter than the hydrodynamic time scale and our main interest is the radiative output. These two cases can be regarded as the very early and the maximum phases of flares respectively. The continuum emission is then computed for the two models when considering the nonthermal collisional effects by electron beams precipitating from the corona.

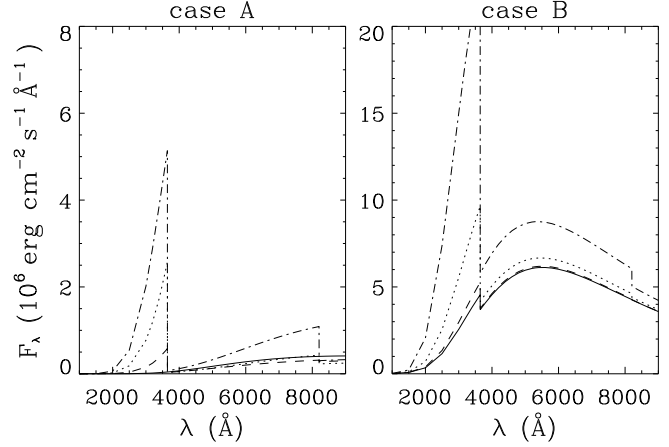


Figure 1. Continuum spectra computed for a quiescent model (case A, left panel) and a flare model (case B, right panel) when considering the nonthermal collisional effects by precipitating electron beams. The energy fluxes, \mathcal{F}_1 , of the beams are 0 (solid line), 10^{10} (dashed line), 10^{11} (dotted line), and 10^{12} (dash-dotted line) $\text{erg cm}^{-2} \text{s}^{-1}$. For all cases, the low-energy cut-off, E_1 , is 20 keV, and the power index, δ , is 3.

As an example, Fig. 1 plots the continuum spectra computed for both models in the presence of electron beams with a low-energy cut-off $E_1 = 20$ keV and a power index $\delta = 3$ but different energy fluxes $\mathcal{F}_1 = 0, 10^{10}, 10^{11}$, and 10^{12} $\text{erg cm}^{-2} \text{s}^{-1}$. It clearly shows that the bombardment of an electron beam leads to a dramatic increase of the continuum emission in the Balmer continuum region ($\lambda < 3646$ Å). The flux at the Paschen continuum region ($\lambda < 8204$ Å) changes to a relatively smaller extent. Therefore, a strong Balmer jump appears in the computed spectra which has not been observed (see also, Hawley & Fisher 1992). Mauas & Falchi (1996) proposed that the merging of higher Balmer lines results in a pseudo-continuum which can smear out the Balmer jump. In the present case, the nonthermal electrons are expected to strengthen the Balmer lines as well (Fang et al. 1993). Thus, the merging effect could be even more important here. In addition, the Doppler effect due to velocity fields of several hundreds of km s^{-1} possibly existing in the flaring atmosphere (e.g. Houdebine et al. 1993), and the line blanketing effect, which is not considered here, can also help to lessen the amplitude of the Balmer jump.

3.1 Enhanced continuum emission and the spectral colour

To make a comparison with observations, we extract the fluxes at $\lambda = 3600$ and 4400 Å, which lie in the centre of the Johnson *U* and *B* bands, respectively, and then compute the following parameters,

$$\Delta U' = -2.5 \log[F_{3600,f}/F_{3600,q}], \quad (13)$$

$$\Delta B' = -2.5 \log[F_{4400,f}/F_{4400,q}], \quad (14)$$

and

$$\Delta(U' - B') = \Delta U' - \Delta B'. \quad (15)$$

In the above equations, a subscript ‘f’ refers to the flaring status (a quiescent/flare atmospheric model with a precipitating electron beam), while ‘q’ to the pre-flare status (a

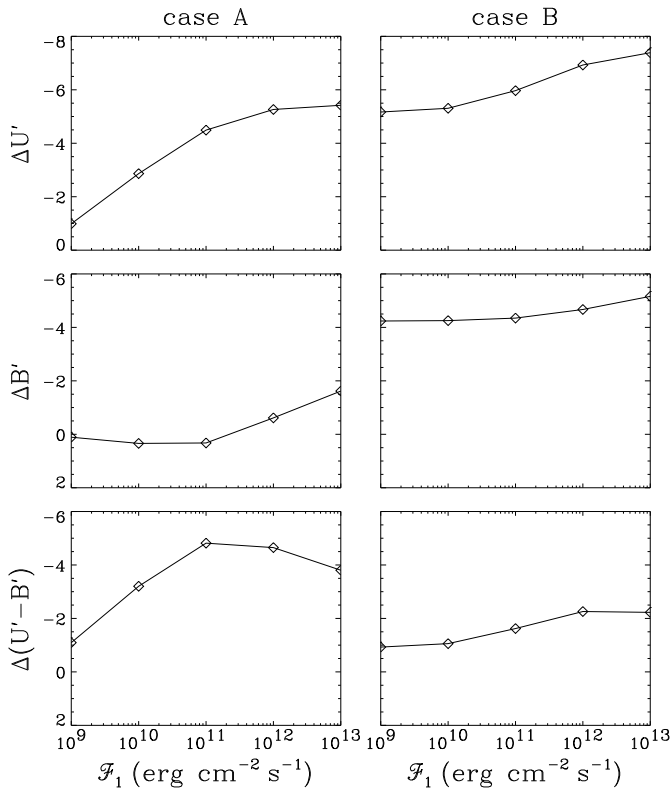


Figure 2. Computed parameters of $\Delta U'$, $\Delta B'$, and $\Delta(U' - B')$ in dependence of the energy flux of the precipitating electron beam. For all cases, the low-energy cut-off, E_1 , is 20 keV, and the power index, δ , is 3.

quiescent atmospheric model only). A prime means that the parameters are defined at fixed wavelength points instead of broad bands usually used in observations. Thus, the results can only be considered as exploratory.

Fig. 2 displays the computed parameters versus the electron beam fluxes. One finds that in the case of a large beam flux, pure nonthermal effects can help to raise the emission at $\lambda = 3600 \text{ \AA}$ by two orders of magnitude. For example, if \mathcal{F}_1 reaches $\sim 10^{12} \text{ erg cm}^{-2} \text{ s}^{-1}$, one obtains an enhancement corresponding to $\Delta U' \sim -5.3$ (case A). Adopting a heated atmospheric model with the same electron beam yields further $\Delta U' \sim -6.9$ (case B). This means that in the U band, the nonthermal effects could dominate over the effect of temperature rise (the thermal effect) in producing the continuum emission. Pagano et al. (1997) reported on a large flare occurring on a dMe star G 102-21, which had a U band enhancement of ≈ 7.3 mag. Taking into account the different pre-flare atmospheric conditions, we conclude that the U band emission in this flare can be qualitatively explained in terms of nonthermal effects.

Under the current framework that the electron beam originates in the corona, it is conceivable that the Paschen continuum is less affected by the electron beam since it is formed in deeper layers than the Balmer continuum. Judging from Fig. 2, the thermal contribution to the emission in the B band may remain to prevail over that due to nonthermal effects. For an electron beam with $\mathcal{F}_1 \sim 10^{12} \text{ erg cm}^{-2} \text{ s}^{-1}$, $\Delta B'$ is computed to be ~ -0.6 and -4.7 in cases A and B, respectively. The latter value is closer to the observations by

Pagano et al. (1997), who obtained a B band enhancement of ≈ 3.9 mag.

Due to the greatly enhanced emission in the U band, the computed spectral colour appears very blue. The colour change, $\Delta(U' - B')$, is computed to show the difference of relative enhancements at U' and B' wavelengths. In case A, this parameter varies in a broad range. The bluest colour, $\Delta(U' - B') \sim -4.8$, appears when $\mathcal{F}_1 \sim 10^{11} \text{ erg cm}^{-2} \text{ s}^{-1}$. The colour turns less blue if further increasing the values of \mathcal{F}_1 . Thus, the observed colour change, $\Delta(U - B) \approx -3.4$ (Pagano et al. 1997), is easy to be reproduced. In case B, however, the spectra are contaminated by the thermal effect, the bluest colour of which is shown to be $\Delta(U' - B') \sim -2.3$ for electron beams considered here. The different results in these two cases imply that the observed blue colour is very likely of nonthermal origin. A pure thermal model is practically hard to reproduce such a blue colour.

Finally, it is worth noting that an electron beam can produce a return current instability when its flux exceeds some critical value. According to the formula derived by Aboudarham & Hénoix (1986), we have found that electron beams with $\mathcal{F}_1 \sim 10^{12} \text{ erg cm}^{-2} \text{ s}^{-1}$ are stable in the corona of the flare model while they are only marginally stable in the corona of the quiescent model. Hence, a favourable situation for the existence of such a large energy flux includes a relatively higher preflare coronal pressure and a harder spectrum of the electron beam (a smaller δ and/or a larger E_1).

3.2 The cause of a continuum dimming

A continuum dimming is produced at the Paschen continuum (B' and V' wavelengths) in the case of a cool atmosphere (case A) bombarded by an electron beam with a moderate energy flux ($\mathcal{F}_1 \lesssim 10^{11} \text{ erg cm}^{-2} \text{ s}^{-1}$). However, such a darkening switches quickly to a brightening with increasing values of \mathcal{F}_1 . In the present models, we cannot produce a dimming at the Balmer continuum.

The continuum dimming results from attenuation of the photospheric radiation by an enhanced opacity in the lower chromosphere and the temperature minimum region. Non-thermal ionisation of hydrogen atoms overpopulates the ambient electrons, leading to an enhanced H^- opacity. Therefore, the magnitude of the depression depends sensitively on the electron energy, which determines the electron penetration depth. Fig. 3 illustrates the effect on the continuum dimming at $\lambda = 4400 \text{ \AA}$ of varying the low-energy cut-off, while keeping the energy flux of the electron beams unchanged. It clearly shows a positive dependence of the magnitude of the dimming on the electron energy.

In observations, the U band comprises a part of the Paschen continuum. Thus, we think that the observed continuum dimming could be related to an electron beam bombarding a relatively cooler atmosphere. This is likely to occur in the early phase of flares. In conclusion, the nonthermal effects could at least partly, if not fully, account for the continuum dimming observed in some stellar flares (e.g. Hawley et al. 1995).

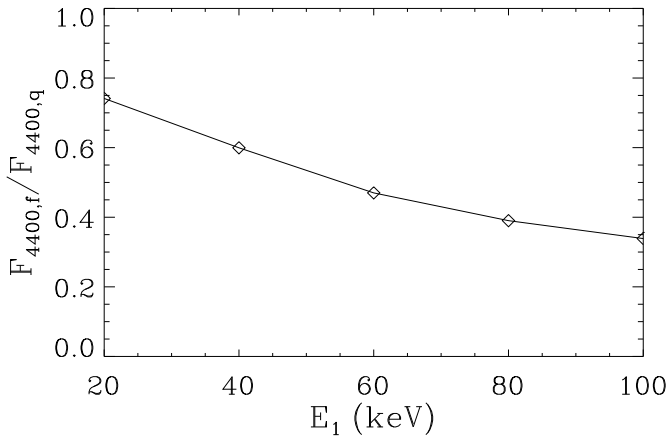


Figure 3. Computed continuum dimming, $F_{4400,f}/F_{4400,q}$, in dependence of the low-energy cut-off of the precipitating electron beam. For all cases, the energy flux, \mathcal{F}_1 , is 10^{11} erg cm $^{-2}$ s $^{-1}$, and the power index, δ , is 3.

3.3 Interpretations of the results

To understand more clearly the above results, we give in Fig. 4 the height distributions of the source function, optical depth and the contribution function per unit geometrical depth,

$$dF_\lambda/dz = 2\pi \int_0^1 j_\lambda e^{-\tau_\lambda/\mu} d\mu, \quad (16)$$

at $\lambda = 3600$, and 4400 Å for case A. It shows that the nonthermal effects can raise both the source function and the opacity to a large extent in the chromosphere. Thus, the chromospheric contribution to the emergent flux gradually increases while the photospheric contribution decreases with increasing electron beam flux. Whether the continuum brightens or darkens is then determined by the competition of these two factors.

4 CONCLUSIONS

If stellar flares result from the reconnection of magnetic fields, analogously to solar flares, electrons and/or protons could be accelerated at the reconnection site and then precipitate into the lower atmosphere. The nonthermal collisional excitation and ionisation of ambient hydrogen atoms by these electrons lead to an enhancement of the source function and opacity in the atmosphere. The chromospheric contribution to the continuum emission rises rapidly, producing a spectrum with a very blue colour. By employing an atmospheric model for an M dwarf star, AD Leo, at quiescent state (Mauas & Falchi 1994), we have computed the continuum spectra for various electron beams bombarding the atmosphere from the corona. The results show that an intense electron beam with an energy flux, for example, $\mathcal{F}_1 \sim 10^{12}$ erg cm $^{-2}$ s $^{-1}$ can produce a continuum flux at $\lambda = 3600$ Å (Balmer continuum) two orders of magnitude greater than the quiescent value. The U band brightening and, in particular, the $U - B$ colour are roughly comparable with observed values for a typical large flare. Adopting an atmospheric model for the flaring state can further raise

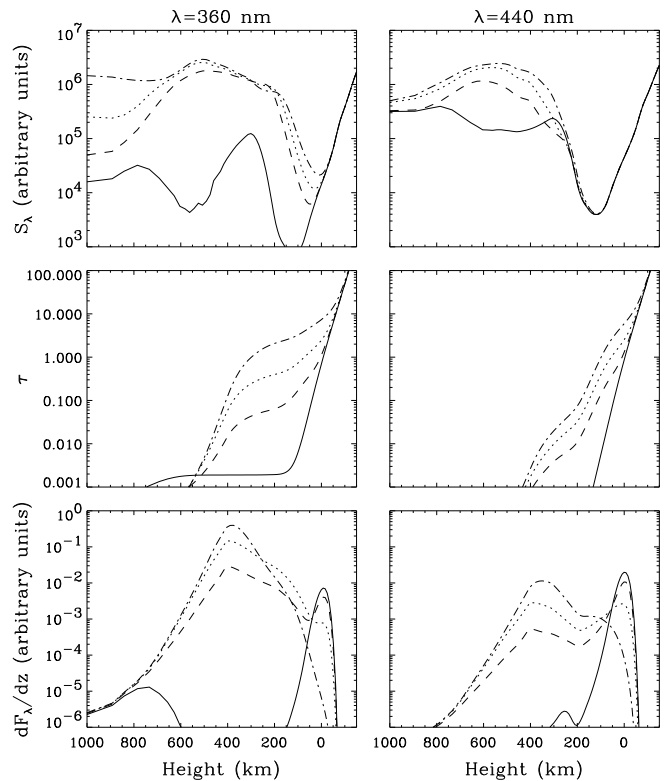


Figure 4. Height distributions of the source function, optical depth and the contribution function at $\lambda = 3600$, and 4400 Å for case A. The energy fluxes, \mathcal{F}_1 , of the electron beams are 0 (solid line), 10^{10} (dashed line), 10^{11} (dotted line), and 10^{12} (dash-dotted line) erg cm $^{-2}$ s $^{-1}$. For all cases, the low-energy cut-off, E_1 , is 20 keV, and the power index, δ , is 3.

the continuum flux and can better account for the B band enhancement. However, it yields a spectral colour incomparable with observations. This implies that the nonthermal effects may play the chief role in powering the continuum emission in some stellar flares.

Computations also predict a continuum dimming at the Paschen continuum, due to attenuation of the photospheric radiation by an enhanced opacity in the lower chromosphere and the temperature minimum region. This happens in a cool atmosphere bombarded by an electron beam with a moderate energy flux ($\mathcal{F}_1 \lesssim 10^{11}$ erg cm $^{-2}$ s $^{-1}$). This is likely to fit the conditions in the very early phase of flares. The magnitude of the dimming depends positively on the electron energy. We argue that the continuum dips found in observations (e.g. Hawley et al. 1995) could possibly be related to nonthermal electrons of higher energies.

ACKNOWLEDGEMENTS

The authors are very grateful to the referee, Prof. J. C. Brown, for his valuable comments on the manuscript. This work was supported by the Research Fund for the Doctoral Programme of Higher Education and by a grant from the National Natural Science Foundation of China.

REFERENCES

- Abouadarham J., Hénoux J.-C., 1986, *A&A*, 168, 301
 Chambe G., Hénoux J.-C., 1979, *A&A*, 80, 123
 Cram L. E., Mullan D. J., 1979, *ApJ*, 234, 579
 Dennis B. R., Zarro D. M., 1993, *Solar Phys.*, 146, 177
 Ding M. D., Fang C., 1996, *A&A*, 314, 643
 Doyle J. G., Houdebine E. R., Mathioudakis M., Panagi P. M.,
 1994, *A&A*, 285, 233
 Emslie A. G., 1978, *ApJ*, 224, 241
 Fang C., Ding M. D., 1995, *A&AS*, 110, 99
 Fang C., Hénoux J.-C., Gan W. Q., 1993, *A&A*, 274, 917
 Grinin V. P., 1983, in Byrne P. B., Rodonò M., eds, *Activity in
 Red Dwarf Stars*. Reidel, Dordrecht, p. 613
 Gurzadyan G. A., 1980, *Flare Stars*, Pergamon Press, Oxford
 Haisch B., Strong K. T., Rodonò M., 1991, *ARA&A*, 29, 275
 Hawley S. L., Fisher G. H., 1992, *ApJS*, 78, 565
 Hawley S. L., Pettersen B. R., 1991, *ApJ*, 378, 725
 Hawley S. L. et al., 1995, *ApJ*, 453, 464
 Hénoux J.-C., Abouadarham J., Brown J. C., van den Oord G. H.
 J., van Driel-Gesztelyi L., Gerlei O., 1990, *A&A*, 233, 577
 Hénoux J.-C., Fang C., Gan W. Q., 1993, *A&A*, 274, 923
 Houdebine E. R., Doyle J. G., 1994, *A&A*, 289, 169
 Houdebine E. R., Stempels H. C., 1997, *A&A*, 326, 1143
 Houdebine E. R., Foing B. H., Doyle J. G., Rodonò M., 1993,
A&A, 274, 245
 Houdebine E. R., Doyle J. G., Kościelicki M., 1995, *A&A*, 294,
 773
 Houdebine E. R., Mathioudakis M., Doyle J. G., Foing B. H.,
 1996, *A&A*, 305, 209
 Machado M. E. et al., 1986, in Neidig D. F., ed., *The Lower Atmo-
 sphere of Solar Flares*. National Solar Observatory, Sunspot,
 NM, p. 483
 Mauas P. J. D., Falchi A., 1994, *A&A*, 281, 129
 Mauas P. J. D., Falchi A., 1996, *A&A*, 310, 245
 Mullan D. J., 1975, *A&A*, 40, 41
 Neidig D. F., Kiplinger A. L., Cohl H. S., Wiborg P. H., 1993,
ApJ, 406, 306
 Pagano I., Ventura R., Rodonò M., Peres G., Micela G., 1997,
A&A, 318, 467
 Short C. I., Doyle J. G., 1998, *A&A*, 336, 613
 van den Oord G. H. J. et al., 1996, *A&A*, 310, 908
 van Driel-Gesztelyi L., Hudson H. S., Anwar B., Hiei E., 1994,
Solar Phys., 152, 145